Improving on numerical simulations of nonlinear CMB anisotropies

2015 J. Phys.: Conf. Ser. 600 012027

(http://iopscience.iop.org/1742-6596/600/1/012027)

Journal of Physics: Conference Series **600** (2015) 012027 doi:10.1088/1742-6596/600/1/012027

Improving on numerical simulations of nonlinear CMB anisotropies

Màrius Josep Fullana i Alfonso[1], Josep Vicent Arnau i Córdoba[2], Robert J. Thacker[3], Hugh M.P. Couchman[4] and Diego P. Sáez Milán[5]

[1] IMM, Universitat Politècnica València, Camí de Vera, s/n 46022 València
[2] DMA, Universitat de València, Dr. Moliner 50, 46100 Burjassot, Spain
[3] DAP, St. Mary's University, Halifax, Nova Scotia, B3H 3C3 Canada
[4] DPA, McMaster University, 1280 Main St. West, Hamilton, Ontario, L8S 4M1 Canada
[5] DAA, Universitat de València, Dr. Moliner 50, 46100 Burjassot, Spain

E-mail: mfullana@mat.upv.es

Abstract. An Adaptative-Particle-Particle-Particle-Mesh code (HYDRA) plus a ray-tracing procedure was used in [1] to perform an exhaustive analysis of the weak lensing anisotropy. Other nonlinear Cosmic Microwave Background anisotropies, such as the Rees-Sciama and the Sunyaev-Zel.dovich effects are also being studied by using the same tools. Here we present some advances in our study of these nonlinear anisotropies. The primary advance is due to the use of better simulations with greater particle densities and appropriate softening, although other parameters have also been adjusted to get better estimates. Thus, we improve on a previous paper [2] where the Rees-Sciama effect was studied with Particle-Mesh simulations. We focus particular attention on the resolution improvement and its consequences.

1. Introduction

For almost a decade, our research team has been working on the computation of Cosmic Microwave Background (CMB) anisotropies using N-body numerical codes (in references [1] to [10], the reader may find a detailed description of the work we have done). The CMB anisotropies computed are those contributing to the CMB angular power spectrum at high ℓ. These anisotropies are mainly produced by nonlinear inhomogeneities placed at large enough distances from the observer; so, these inhomogeneities subtend small angular scales and contribute to large ℓ multipoles. We deal with the anisotropies due to weak lensing (WL), Rees-Sciama (RS) and Sunyaev-Zel'dovich (SZ).

Our initial studies used Particle-Mesh (PM) codes which have low resolution (see [2] to [6]). The resulting calculations were improved by using Adaptative-Particle-Particle-Particle-Mesh (AP3M) codes with more resolution (see [1] and [7] to [10]). We first used the sequential AP3M code HYDRA [7] in dark matter only mode and computed RS and WL CMB anisotropies. Afterwards, a Hydra AP3M parallel code was used to do the same estimates with more resolution and greater boxes [1]. Now, we are moving CMB photons along the simulation boxes of a Hydra AP3M parallel code with baryons [9, 10]. As might be expected, for similar boxes and resolution, the RS and WL CMB anisotropy estimations with baryons give almost the same results as those obtained without baryons [9]. The calculation of the SZ effect is also being performed [10]. Our underlying goal is to compute the RS, WL and SZ effects at the same time, to study

the coupling of these three contributions to the CMB anisotropy will be analyzed. The peculiar gravitational potential, its gradients, the electron number density, and other necessary quantities are calculated and used at every time step of the Hydra simulation evolution. The main scope of this paper is to show how the results of some computations improve as the resolution is increased.

2. Mapping

Here we describe the quantities that are computed at every step of the code evolution to calculate CMB anisotropies.

For WL, small unlensed maps of CMB temperature contrasts, $\Delta T/T$, must be constructed to be subsequently deformed by lensing. In order to deform the unlensed maps, the lens deviations corresponding to a set of directions, covering an appropriate region of the sky, must be calculated. These deviations are the quantities:

$$\vec{\delta} = -2 \int_{\lambda_e}^{\lambda_0} W(\lambda) \vec{\nabla}_\perp \phi \; d\lambda \; , \tag{1}$$

where $\vec{\nabla}_\perp \phi = -\vec{n} \wedge \vec{n} \wedge \vec{\nabla} \phi$ is the transverse gradient of the peculiar gravitational potential, and $W(\lambda) = (\lambda_e - \lambda)/\lambda_e$. The variable λ is

$$\lambda(a) = H_0^{-1} \int_a^1 \frac{db}{(\Omega_{m0} b + \Omega_\Lambda b^4)^{1/2}} \; . \tag{2}$$

H_0, Ω_m, and Ω_Λ being the Hubble constant, and the density parameters of matter and vacuum, respectively. By using these formulas, the temperature contrasts $\Delta T/T$, and the C_ℓ coefficients due to WL may be computed (see [1] for a detailed description of the method).

The RS contribution is:

$$\frac{\Delta T}{T}(\vec{n}) = 2 \int_{\lambda_e}^{\lambda_0} W(\lambda) \; \frac{\partial \phi}{\partial \lambda} \; d\lambda \; , \tag{3}$$

where ϕ is the peculiar gravitational potential, $W(\lambda) = (\lambda_e - \lambda)/\lambda_e$, and λ is given in Eq. (2). (See [2] for details).

The temperature contrast of the SZ thermal effect is:

$$\frac{\Delta T}{T}(\vec{n}) = -2 \; \frac{\sigma_T}{m_e c^2} \int_{l_i}^{l_0} n_e \; k \; (T_e - T_{CMB}) \; dl \; , \tag{4}$$

Finally, for SZ kinematic contribution one has:

$$\frac{\Delta T}{T}(\vec{n}) = - \; \frac{\sigma_T}{c} \int_{l_i}^{l_0} n_e \; v_r \; dl \; , \tag{5}$$

where the subscript e refers to electrons. (See [10] for more details).

3. Algorithm to compute the integrals

The steps we follow to compute the above integrals are now described. Various steps are related with the implementation of our ray-tracing procedure. For a detailed description of this procedure see for instance [4]. Main steps:

(i) Decide the preferred directions.

(ii) Assume the Born approximation, and use the photon step distance Δ_{ps} to determine all the evaluation positions and times on the geodesics. Evaluations are performed inside the simulation volume, from $z_i = 6$ down to the final redshift.

(iii) Associate test particles (without mass) to each of these positions and times.

(iv) For SZ, evaluate the radial component of the peculiar velocity, the number density, and the temperature of the electron gas, in the position and time corresponding to each test particle.

(v) In these positions and times (test particles), evaluate the potential and its gradient (force), using the long-range FFT component and short-range PP correction, as it is done in the HYDRA code.

(vi) During the FFT convolution for the test particles, eliminate contributions from scales larger than $42h^{-1}$ Mpc; namely, remove the signal from wavenumbers $k \leq 0.15h$ Mpc^{-1}. This procedure is required by our ray-tracing method.

(vii) If the evaluation time for a point on a null geodesic lies between two time-steps, calculate a linear interpolation of the physical quantities from the time-steps that straddle the correct time.

4. Hydra Simulations

All the simulations, have been performed in the framework of a concordance model with the following parameters: $h = 0.7$, $\Omega_b = 0.046$, $\Omega_d = 0.233$, $\Omega_\Lambda = 0.721$, $\tau = 0.084$ and $\sigma_8 = 0.817$. The power spectrum of the scalar (adiabatic) energy density perturbations, and the CMB angular power spectrum, necessary for simulations, were calculated using the latest generation of the CMBFAST code. No tensor modes have been considered.

The CMB photons move along specially chosen oblique paths through the simulation box; so, the usual traslations and rotations of boxes are not necessary to avoid periodic effects. In this way, the periodicity inside the box volume ensures that there are no discontinuities in the matter field where photons cross from box to box. We take care to ensure that, for the chosen paths, periodicity effects become negligible. In order to minimize these effects, the photons must cross consecutive boxes through statistically independent regions, which requires: (i) *preferred directions* leading to large enough distances between these regions and, (ii) a suitable cutting to avoid large scale spatial correlations ($k < 0.15h\ Mpc^{-1}$ or spatial scales $r_c > 60h^{-1}Mpc$) between the above distant regions. In [1], a detailed description of the parameters involved in the Hydra code may be found.

5. Results and Discussion

We have focused our attention on the resolution of our codes for CMB anisotropy estimations. Advances on simulations of structure formation have allowed us the design of better codes with more resolution, which led to more accurate results. Our predictions have been compared with previous ones and with observational data (see [1] and [8]). Here, we present some plans to improve on our estimates of the SZ and WL angular power spectra, and some new results relative to the RS effect.

5.1. SZ signal

As it was explained in [10], the computation of the thermal SZ (the largest effect at large enough ℓ) and the kinematic SZ signals could be done in two different ways: (1) the integrands in Eqs. (4) and (5) are computed, for the positions and times of the test particles, in the same way as it is done for real particles in the original Hydra code. This procedure would take a long CPU time, but it is the most coherent one and, (2) we could look for a lower CPU cost by using suitable approaches to estimate the integrands. This second alternative has not led to robust enough codes [10] for the approaches used up to now; nevertheless, new approaches might be designed. The coherent –long CPU time– method (1) is being implemented.

5.2. WL signal

A detailed study of the WL effect was published in [1], where simulations with different mass and space resolutions were considered; so, it was shown that results are better for greater resolutions. Low resolutions lead to Poisson discretization errors producing a wrong power excess at very small angular scales. Our best resolution was reached for simulations of 512^3 particles in boxes of $256h^{-1}\ Mpc$. Thus, a signal higher than that obtained in previous estimates was obtained. Actually, for $4000 < \ell < 7000$, we found a signal of $2.0 \pm 0.4\ \mu$K, which is $\sim 1.4\mu K$ higher than that found elsewhere (see [1] and references cited therein). Although our best resolutions seem to be good enough to avoid discretization errors, new simulations with higher resolutions are desirable to discuss if Poisson errors are really negligible against the high WL signal we estimated.

For resolutions greater than the best one in [1], the presence of baryons should begin to influence the predicted WL power, and simulation errors –in general– may depend on the code structure through various parameters and conditions, On account of these facts, we have tried to improve on our simulations by using a Hydra code with baryons. Two ways may be followed; in the first one, the same code –without baryons– as in [1] is used, but a better resolution is achieved by using 1024^3 (a power of two is required) particles in $256h^{-1}\ Mpc$ boxes. In the second way, a new Hydra code including baryons is run for 2×640^3 particles evolving in a $200h^{-1}\ Mpc$ box. Various technical problems must be solved before these simulations can be evolved to low enough redshifts. Further research is in progress with the essential aim of improving on the results of paper [1] and looking for the imprint of baryons in the WL spectra.

5.3. RS signal

Although the Integrated Sachs-Wolfe effect and the RS one may be both calculated by using Eq. (3), according to paper [2], these effects may be properly separated. The RS signal is very small. As can be seen in Fig. 1, this signal reaches a maximum smaller than 1 μK for an ℓ value of the order of 10^3. Similar results were also found in [2]. Although the RS signal is dominated either by primary CMB anisotropies or by the SZ effect, it might be detected, in future, from accurate CMB anisotropy measurements plus complete extended maps of nonlinear structures (clusters, superclusters, and so on). Detection could be achieved by measuring correlations between the distribution of these structures and the CMB anisotropy maps.

Some years ago, the RS angular power spectrum was estimated [2] by using our ray-tracing procedure and a Particle Mesh (PM) N-body code designed by V. Quilis and one of us (DPSM). The main features of this code can be found in [2]. It was adapted by us for CMB applications. Using 512^3 particles in boxes of $512h^{-1}\ Mpc$, the spatial resolution of the PM code is only $\sim 350kpc$. In order to obtain better results a greater resolution would be necessary. Hydra codes can be adapted to include our ray tracing method; so, the RS effect may be simulated with much greater resolutions.

The PP part of the Hydra algorithm allows us to get good space and mass resolutions. Neither a too large number of particles nor too small simulation boxes are necessary. In the simulations performed to built up Fig. 1 (hereafter simulations of reference), 256^3 particles evolve inside boxes with a size of $512h^{-1}\ Mpc$. The mass of the dark matter particles is $8.8 \times 10^{11}\ M_\odot$. Moreover, a Plumber softening $S_p = 6h^{-1}\ kpc$ has been chosen and, consequently, the spatial resolution is $\sim 5S_p = 30h^{-1}\ kpc$. This resolution is around ten times greater than that of the PM code used in [2]. These large resolutions are achieved in spite of the fact that: (i) both codes use the same boxes and, (ii) the Hydra code evolves less particles (256^3) than the PM one (512^3). We use the same Hydra code without baryons as in [1], where simulations with the same characteristics led to a good estimate of the WL anisotropy. Finally, the integration step –also called photon step Δ_{ps}– used to perform the integral in Eq. (3) along the background null geodesics is $\Delta_{ps} = 15h^{-1}\ kpc$. Moreover, the number of geodesics is 256^2 (a 4 factor less than

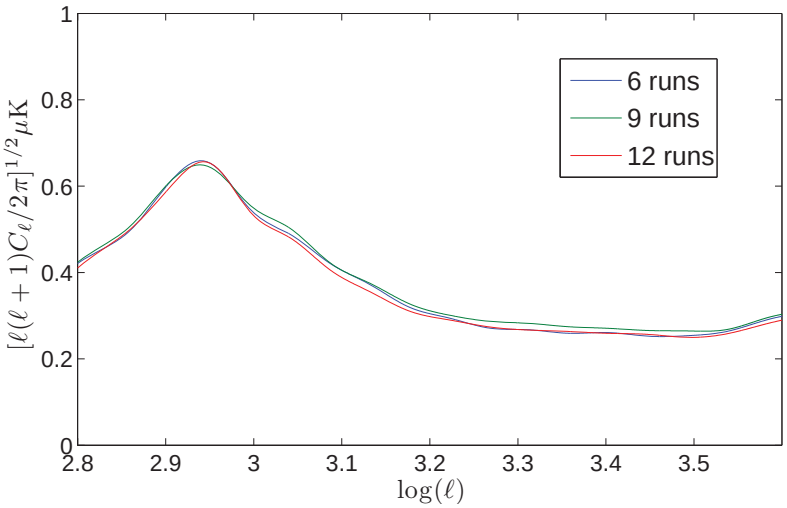

Figure 1. RS power spectrum, in μK, as a function of $\log(\ell)$. Here we plot the mean of 6, 9 and 12 runs estimates. For all cases initial redshift is $z_i = 6$. The number of particles is 256^3 and the box size $512h^{-1}Mpc$.

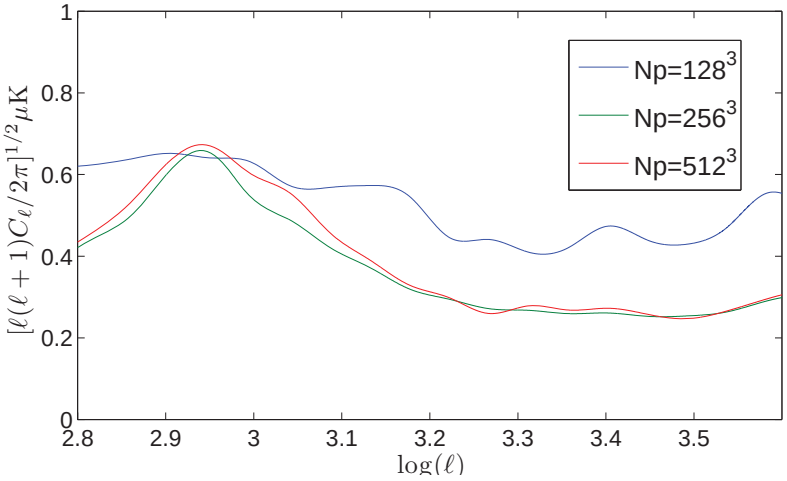

Figure 2. RS power spectrum, in μK, as a function of $\log(\ell)$. Blue, green, and red lines correspond to averages obtained with six simulations of 128^3, 256^3 and 512^3 particles, respectively. For all cases the initial redshift is $z_i = 6$ and the box size $512h^{-1}Mpc$.

that in [2]) and the angular resolution of the RS maps is $1.17'$.

From a unique simulation, it is not possible to obtain an accurate enough RS spectrum; in other words, a unique RS map is not a large enough statistical sample. A certain number of simulations must be run. In Fig. 1, the RS power spectra obtained by averaging over 6, 9 and 12 runs are plotted. The three spectra are very similar and, consequently, six runs are sufficient to get a good enough RS spectrum; however, about 30 runs were necessary in [1] –with a PM code– to get comparable results.

We have studied the impact of mass resolution by using simulations with 128^3, 256^3 and

512^3 particles in boxes with a size of $512h^{-1}\ Mpc$. The remaining parameters are assumed to be identical to those of the reference simulations, excepting the masses of the dark matter particles, which are 7.0×10^{12}, and $1.1 \times 10^{11}\ M_\odot$ for 128^3 and 512^3 particles, respectively. In Fig. 2, the RS angular power spectra corresponding to the three above simulations are plotted. Evidently, the simulation with 128^3 particles does not have enough resolution, and the resulting signal does not appear adequately resolved. However, the reference simulations (256^3 particles) and those evolving 512^3 particles lead to very similar RS spectra, which we take as suggesting the signal is converging with resolution. The simulations with the best resolution (512^3 particles) give a sligthly higher peak. Since these two spectra have been obtained by averaging six simulations, this small power excess should be real, since according to our discussion about Fig. 1, it is evident that the mentioned excess should not sensibly change as the number of averaged solutions exceeds six.

Acknowledgments

This work has been supported by the Spanish Ministry of *Economía y Competitividad*, MICINN-FEDER project FIS2012-33582. Calculations have been made using the Lluís Vives Computer of Universitat de València. We are greatful to the working team of the Servei d'Informàtica de la Universitat de València for their useful help.

References

[1] Fullana M J, Arnau J V, Thacker R J, Couchman, H M P and Sáez D 2010 *ApJ* **712** 367
[2] Puchades N, Fullana M J, Arnau J V and Sáez D 2006 *MNRAS* **370** 1849
[3] Fullana M J and Sáez D 2006 *Proceedings of the Sixth International Symposium "Frontiers of Fundamental and Computational Physics" (Udine)* ed B G Sidharth et al (Springer, The Netherlands) p 115
[4] Sáez D, Puchades N, Fullana M J and Arnau J V 2006 *Proceedings of the International Conference "CMB and Physics of the Early Universe" (Ischia)* ed G de Zotti (PoS) p058
[5] Sáez D, Puchades N, Fullana M J and Arnau J V 2006 *A century of relativity physics, Proceedings o f the 28th Spanish Relativity Meeting (Oviedo)* ed L Mornas and J Díaz Alonso (AIP Conference Proceedings vol 841 Melville New York) p 594
[6] Fullana M J and Sáez D 2007 *Frontiers of Fundamental and Computational Physics (FFP8) (Madrid)* ed B G Sidhart, A Alfonso-Faus and M J Fullana i Alfonso (AIP Conference Proceedings vol 905 Melville New York) p 13
[7] Fullana M J, Arnau J V and Sáez D 2008 *Frontiers of Fundamental and Computational Physics: 9th International Symposium (Udine and Trieste)* ed B G Sidharth et al (AIP Conference Proceedings vol 1018 Melville New York) p 80
[8] Fullana M J, Arnau J V, Thacker R J, Couchman, H M P and Sáez D 2012 *Frontiers of Fundamental Physics: The Eleventh International Symposium (Paris)* ed J Kouneiher et al (AIP Conference Proceedings vol 1446 Melville New York) p 252
[9] Fullana M J, Arnau J V, Thacker R J, Couchman, H M P and Sáez D 2014 *Frontiers of Fundamental Physics and Physics Education Research 12th edition (Udine)* ed B G Sidharth et al (Springer Proceedings in Physics vol 145 Switzerland) p 188
[10] Fullana M J, Arnau J V, Thacker R J, Couchman, H M P and Sáez D 2014 *Progress in Mathematical Relativity, Gravitation and Cosmology, Proceedings of the Spanish Relativity Meeting ERE2012, (Guimarães)* ed A García-Parrado et al (Springer Proceedings in Mathematics and Statistics vol 60 Springer-Verlag Berlin Heidelberg) p 277